# Essential role of immobilized chemokine CXCL12 in the regulation of the humoral immune response

Aleksandr Barinov[a,b,1], Lingjie Luo[c,d,1], Pamela Gasse[c,d,1], Vannary Meas-Yedid[e,f], Emmanuel Donnadieu[g,h,i], Fernando Arenzana-Seisdedos[c,d,j,2], and Paulo Vieira[a,b,2]

[a]Department of Immunology, Unité Lymphopoïèse, Institut Pasteur, 75015 Paris, France; [b]INSERM U1223, 75015 Paris, France; [c]Department of Virology, Unité de Pathogénie Virale, Institut Pasteur, 75015 Paris, France; [d]INSERM U819, 75015 Paris, France; [e]Department of Cell Biology & Infection, Unité d'Analyse d'Images Biologiques, Institut Pasteur, 75015 Paris, France; [f]CNRS UMR 3691, 75015 Paris, France; [g]Institut Cochin, INSERM U1016, 75014 Paris, France; [h]CNRS UMR 8104, 75014 Paris, France; [i]Université Paris Descartes, Sorbonne Paris Cité, 75006 Paris, France; and [j]Institut Pasteur de Shanghai, Chinese Academy of Sciences, 200032 Shanghai, China

Edited by Jason G. Cyster, University of California, San Francisco, CA, and approved January 13, 2017 (received for review July 20, 2016)

**Chemokines control the migration of a large array of cells by binding to specific receptors on cell surfaces. The biological function of chemokines also depends on interactions between nonreceptor binding domains and proteoglycans, which mediate chemokine immobilization on cellular or extracellular surfaces and formation of fixed gradients. Chemokine gradients regulate synchronous cell motility and integrin-dependent cell adhesion. Of the various chemokines, CXCL12 has a unique structure because its receptor-binding domain is distinct and does not overlap with the immobilization domains. Although CXCL12 is known to be essential for the germinal center (GC) response, the role of its immobilization in biological functions has never been addressed. In this work, we investigated the unexplored paradigm of CXCL12 immobilization during the germinal center reaction, a fundamental process where cellular traffic is crucial for the quality of humoral immune responses. We show that the structure of murine germinal centers and the localization of GC B cells are impaired when CXCL12 is unable to bind to cellular or extracellular surfaces. In such mice, B cells carry fewer somatic mutations in Ig genes and are impaired in affinity maturation. Therefore, immobilization of CXCL12 is necessary for proper trafficking of B cells during GC reaction and for optimal humoral immune responses.**

CXCL12 | humoral immune responses | germinal center reaction

Chemokines control the migration of a large array of cells and, as a consequence, regulate cell function and homeostasis in many tissues (1). In particular, they regulate the migration and positioning of lymphocytes in secondary lymphoid organs (2). Besides specific signaling delivered by engagement of specific receptors on cell surfaces, the function of chemokines also depends on interactions between nonreceptor binding domains and the glycanic-glycosaminoglycan (GAG) moiety of proteoglycan, particularly heparan sulfate (HS), of the extracellular matrix and cell surfaces (3). This interaction results in immobilization of chemokines and allows the formation of fixed local gradients that, in in vitro models, regulate the synchronous coordination of cell motility (haptotaxis) and integrin-dependent cell adhesion (2). An immobilized, but not free, chemokine is a hallmark of cell signaling (4).

The importance of chemokine immobilization for their function has not been fully addressed, and its relevance has been difficult to evaluate in vivo, given the lack of information on the structure–function relationship of chemokine/HS interactions.

Of the various chemokines, C-X-C motif chemokine 12 (CXCL12) [also known as stromal-cell–derived factor 1 (SDF-1)] has unique structural characteristics because its binding domains, to the receptor C-X-C chemokine receptor type 4 (CXCR4) and to HS, are distinct and nonoverlapping, permitting the separation of their respective functions (5, 6). The interaction with proteoglycans is believed to contribute to CXCL12 activity by enabling the formation of local gradients essential for directed cellular migration (6–8). To investigate how GAG interactions regulate the functions of chemokines in vivo, we have previously developed a mouse strain carrying a mutated form of CXCL12 ($CXCL12^{gagtm}$ mice) where CXCL12/HS interactions are disabled (8). These mice show enhanced serum levels of free CXCL12 and an increased number of circulating leukocytes and $CD34^+$ hematopoietic cells.

CXCL12 is an essential chemokine during development and is critical for the homeostatic regulation of leukocyte trafficking and tissue regeneration (1, 8–10). In addition, CXCL12 plays important roles in the germinal center (GC) reaction during immune responses and is involved in the reentry of long-lived plasma cells in the appropriate bone marrow (BM) niches (11–13).

Antibody responses against foreign antigens start at the T/B border of the follicles of peripheral lymphoid organs (spleen, lymph nodes, Peyer's patches), through interactions between antigen-specific T and B cells (14). Activated B-lymphocytes migrate into the B-cell follicle where they proliferate extensively to form structures called GCs. Two histologically distinct areas are observed in the GC [the dark zone (DZ) and the light zone (LZ)] that depend on the response of GC B cells to opposing gradients of the chemokines CXCL12 (more expressed in the DZ) and CXCL13 (more expressed in the LZ) (11, 15). In the DZ, B cells (centroblasts) proliferate and express the enzyme activation-induced cytidine deaminase (AID), which mediates somatic hypermutation (SHM) of Ig genes (16, 17). In the LZ, where a network of follicular dendritic cells (FDCs) presenting antigen and follicular helper T cells ($T_{FH}$) can be found, B cells (centrocytes) are selected into either the pool of recirculating

## Significance

**High-affinity antibodies confer protective immunity against external antigens and are generated during germinal center (GC) reactions when B-lymphocytes, migrating between the dark zone (DZ) and light zone (LZ) of the GC, accumulate mutations in their immunoglobulin genes and are selected for high affinity to antigen. B cells move between DZ and LZ, guided by gradients of CXCL12 and CXCL13 chemokines. We show that immobilized CXCL12 is essential for the correct positioning of B-lymphocytes during the GC reaction and for the production of high-affinity antibodies. Our results provide fundamental insights into the role of surface-immobilized chemokines, molecules that regulate the migration of many cell types, thus controlling homeostasis in multiple tissues.**

Author contributions: A.B., L.L., P.G., E.D., F.A.-S., and P.V. designed research; A.B., L.L., P.G., V.M.-Y., E.D., F.A.-S., and P.V. performed research; E.D. and F.A.-S. contributed new reagents/analytic tools; A.B., L.L., P.G., V.M.-Y., E.D., F.A.-S., and P.V. analyzed data; and A.B. and P.V. wrote the paper.

The authors declare no conflict of interest.

This article is a PNAS Direct Submission.

[1]A.B., L.L., and P.G. contributed equally to this work.

[2]To whom correspondence may be addressed. Email: paulo.vieira@pasteur.fr or fernando.arenzana-seisdedos@pasteur.fr.

This article contains supporting information online at www.pnas.org/lookup/suppl/doi:10.1073/pnas.1611958114/-/DCSupplemental.

memory B cells or the plasma cell compartment. Available evidence suggests that the GC reaction is maintained by reentry into the DZ of B cells selected in the LZ (18). In the DZ, cells undergo further rounds of proliferation and SHM (11, 19).

In this work, we investigated in vivo the unexplored role of CXCL12 chemokine immobilization during the GC reaction, a fundamental process where cellular traffic determines the quality of humoral immune responses. We studied the recruitment and distribution of B-lymphocytes in the GC, somatic hypermutation of Ig genes, and antibody affinity maturation in CXCL12$^{gagtm}$ mice, where CXCL12 is unable to bind to cellular or extracellular surfaces.

CXCL12$^{gagtm}$ mice have impaired germinal centers, with a majority of them showing poor DZ/LZ segregation. In the few GCs where a clear separation between DZ and LZ can be found, cells in the M phase of the cell cycle are found in the LZ, an aberrant localization for mitotic cells, usually restricted to the DZ compartment. These alterations ultimately result in reduced accumulation of somatic mutations in Ig genes and impaired affinity maturation. Thus, immobilization of CXCL12 is necessary for proper trafficking of B cells during GC reaction and for optimal humoral responses.

## Results

**Magnitude and Kinetics of Germinal Center Reaction in CXCL12$^{gagtm}$ Mice.** The original characterization of CXCL12$^{gagtm}$ mice showed that they develop normally but have increased numbers of circulating CD34$^{+}$ cells (8). We analyzed B-cell subsets in BM and spleen of control and CXCL12$^{gagtm}$ mice and found that only the subset of BM mature recirculating B cells (B220$^{+}$ IgM$^{low}$ IgD$^{+}$) was reduced (Fig. S1*A*). In particular, the frequency and number of BM plasma cells was comparable in both groups (Fig. S1*B*). In the spleen, all subpopulations were normally represented (Fig. S1 *C* and *D*).

To investigate the magnitude and kinetics of the GC reaction, we immunized CXCL12$^{gagtm}$ mice with sheep red blood cells (SRBCs) and followed the splenic GC reaction using expression of CD19, IgD, CD38, CD95, CXCR4, and CD86 (19) to define GC, LZ and DZ B cells (Fig. 1*A*). Forward scatter was used to evaluate the relative size of LZ and DZ cells. DZ cells were slightly larger than LZ B cells in both groups of mice (Fig. 1*A*) whereas the size of the LZ cells was similar in control and mutant mice (Fig. S1*E*). No significant difference in the magnitude or kinetics of the GC reaction was observed (Fig. 1*B*, *Left*). Early in the response, GC B cells constituted 1.3% and 1.5% of B cells in control and mutant mice, respectively, and the peak of the response was on day 7 (9% and 10.5%, respectively), with a reduced GC reaction by day 21 (Fig. 1*B*, *Left*). DZ/LZ ratios were comparable at all time points studied (Fig. 1*B*, *Right*).

**Structure of GC and Analysis of B-Cell Size.** We further investigated the structure of GC and B-cell sizes in their native GC environment by focusing on the localization of centrocytes and centroblasts in the LZ and DZ. For this investigation, we performed histological analysis of splenic GCs at the peak of the response. Analysis of spleen sections of immunized animals revealed heterogeneity in GC structure, with two types of GC observed, based on IgD and FDC-M2 staining patterns of spleen sections: GCs where a clear discrimination between FDC-M2–positive (LZ) and FDC-M2–negative (DZ) GC areas could be seen ("organized" GC), and those where FDC-M2 staining was present throughout the entire GC, with no clear delineation of LZ and DZ ("disorganized" GC) (Fig. 2*A*). A significantly higher fraction of disorganized GCs was observed in CXCL12$^{gagtm}$ mice (Fig. 2*B*). Similar staining patterns were observed when we used antibodies specific for complement receptors 1 and 2 (CD21/CD35) to identify FDCs (Fig. S2*A*). In addition, the IgD-negative area in the follicles correctly

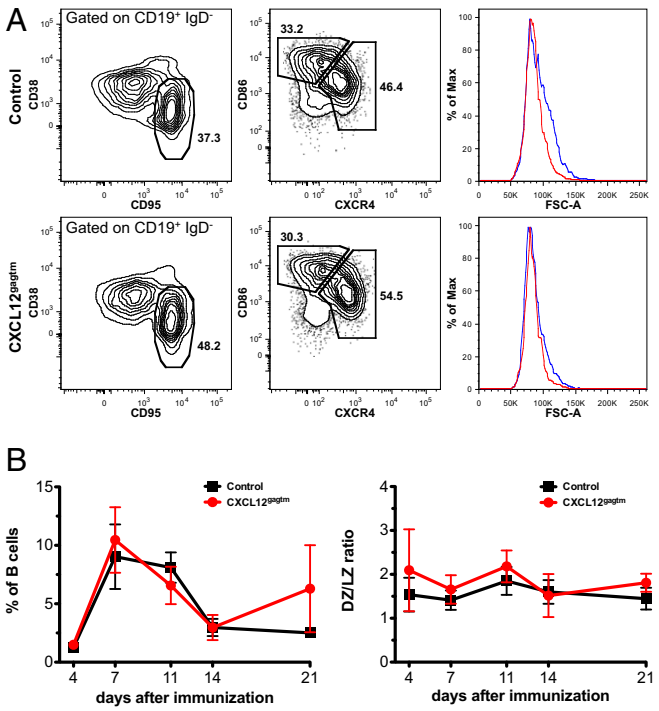


**Fig. 1.** Magnitude and kinetics of germinal center reaction in CXCL12$^{gagtm}$ mice. (*A*) Flow cytometry analysis of splenic GC B cells. (*Left*) The percentage of GC B cells (CD38$^{low}$ CD95$^{high}$) among CD19$^{+}$ IgD$^{-}$ splenocytes from control (*Upper*) and CXCL12$^{gagtm}$ (*Lower*) mice 7 d after SRBC immunization. (*Middle*) Percentage of dark zone (CXCR4$^{high}$ CD86$^{low}$) and light zone (CXCR4$^{low}$ CD86$^{high}$) cells in the GC gate shown on the *Left*. (*Right*) Histograms indicate forward scatter (FSC) profiles of DZ (blue) and LZ (red) cells in the gates shown in *Middle*. Mean FSC intensity in control DZ = 89.3k (±2.6k), LZ = 83.6k (±1.9k) ($n$ = 5, $P$ = 0.0045); mean FSC in CXCL12$^{gagtm}$ DZ = 87.2k (±1.2k), LZ = 84.3k (±1.1k) ($n$ = 5, $P$ = 0.0037). Statistical significance determined by Student's $t$ test. (*B*) Kinetics of the splenic GC reaction after immunization with SRBC (*Left*), and DZ/LZ ratios for the corresponding time points (*Right*) in one representative experiment out of three performed. Data are from 3 to 11 mice per time point and are shown as mean ± SD.

delineates the GC, as determined by Bcl6 staining (Fig. S2*B*), and GC B cells in both control and CXCL12$^{gagtm}$ mice are IgD$^{-}$ (Fig. S2*C*). To quantify the size of the B cells in the LZ and DZ compartments, cell cross-section surface areas in the organized GCs were analyzed in detail. Using a semiautomated framework of ICY software (20) (Fig. S3*A*), individual B-cell surface areas of control and CXCL12$^{gagtm}$ GCs were measured (Fig. 2*C*, *Left*). This analysis revealed that, in control mice, the average area of the B cells was significantly larger in DZ than in LZ, in agreement with prior observations (21, 22). Our data also showed significant differences in the areas of the B cells found in the LZ of control and CXCL12$^{gagtm}$ mice. The surface area of LZ B cells in mutant mice was significantly larger than that in controls whereas no significant differences were found in DZ B cells. The observed cell size differences were not associated with different cellular densities in the LZ compartments because the numbers of B cells per 100 μm$^2$ were similar in control and mutant mice (Fig. S3*B*). The differences were consistent in individual GCs and resulted in a significantly lower ratio of DZ/LZ surface areas in GCs from CXCL12$^{gagtm}$ animals (Fig. 2*C*, *Right*). Taken together, the analyses revealed important alterations in the GC organization and a significant increase in the surface area of LZ cells in the GC of CXCL12$^{gagtm}$ mice. Because cells with the DZ phenotype are generally larger than LZ phenotype cells (Figs. 1*A* and 2*C*) (21, 22), we hypothesized that this result could be due to

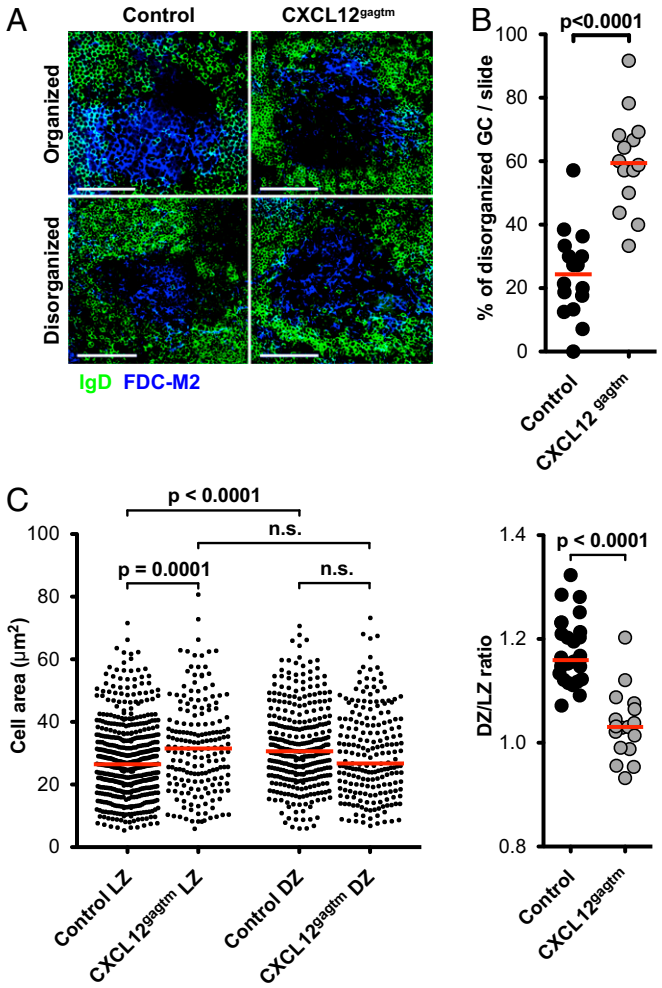


**Fig. 2.** Structure of GC and analysis of B-cell size. (*A*) Representative spleen sections showing organized and disorganized GCs 7 d after immunization with SRBC. Sections were stained with IgD (green) to identify the GC and FDC-M2 (blue) to delineate the LZ. In organized GCs, a clear discrimination between LZ and DZ areas can be made (*Upper*); in disorganized GCs, the discrimination is not evident (*Lower*). One representative GC of each type from eight control and seven CXCL12$^{gagtm}$ mice is shown. (Scale bars: 50 µm.) (*B*) Percentage of disorganized GCs per slide 7 d after immunization. Sixteen slides in eight control mice (202 GC), and 14 slides in seven CXCL12$^{gagtm}$ mice (219 GC) were analyzed blind. Red bars indicate the median values in each group. Statistical significance was determined by Mann–Whitney test. (*C*, *Left*) Surface areas of individual B cells in the LZ and DZ of organized GC. Data from one representative experiment out of two performed. Each point corresponds to one cell in 15 control and 8 CXCL12$^{gagtm}$ GCs from four control and three CXCL12$^{gagtm}$ mice. Statistical significance determined by Student's *t* test. (*Right*) Ratio between DZ/LZ mean surface areas calculated in individual GC. Data are pooled from two independent experiments with a total of 27 control and 17 CXCL12$^{gagtm}$ GCs from eight control and seven CXCL12$^{gagtm}$ mice. Red bars indicate the median values in each group. Statistical significance was determined by Mann–Whitney test.

the mispositioning of centroblasts, secondary to the disrupted binding of CXCL12 to HS in CXCL12$^{gagtm}$ mice.

**Mitotic Cells Are Found in the LZ of GC in Mutant Mice.** To determine whether the positioning of cells with a DZ phenotype is affected in CXCL12$^{gagtm}$ mice, we examined the sites in which GC B cells were undergoing mitosis. It is known that SHM and proliferation occur in the DZ and that cells in G2/M phase of the cell cycle display a DZ phenotype and locate to the DZ compartment (19). As the cells progress from late G2 into prophase, the histone H3 is phosphorylated at positions Ser-10 and Ser-28, with rapid dephosphorylation thereafter (23, 24). Thus, phosphorylated histone H3 is found exclusively in cells in mitosis. We therefore examined GCs for the expression of phospho-histone H3 (PH3), using an antibody specific for phosphorylated H3 at position Ser-10 to visualize the localization of mitotic B cells in GCs (25). In control mice, PH3 Ser-10$^{+}$ cells were found mainly in the DZ compartment (Fig. 3 *A*, *Left* and *B*), confirming that mitosis occurs predominantly in that zone. In contrast, a significantly higher fraction of PH3 Ser-10$^{+}$ cells were found in the LZ when GCs of CXCL12$^{gagtm}$ mice were analyzed (Fig. 3 *A*, *Right* and *B*). Analysis of 658 mitotic cells in 48 individual GCs from CXCL12$^{gagtm}$ animals revealed that PH3 Ser-10$^{+}$ cells were distributed in nearly equal proportions between the DZ and LZ compartments (Fig. 3*B*).

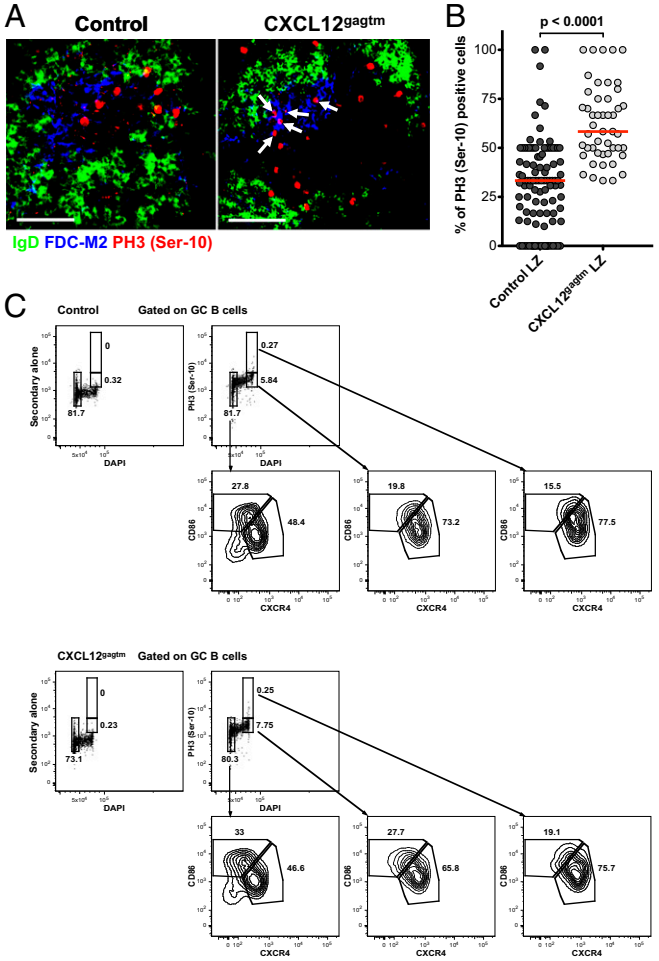


**Fig. 3.** Mitotic cells in the LZ of mutant mice. (*A*) Spleen sections 7 d after SRBC immunization. IgD (green), FDC-M2 (blue), phospho-histone H3 (red). Arrows point to PH3$^{+}$ cells in the LZ. One representative GC from seven control and six CXCL12$^{gagtm}$ mice out of 152 organized GCs analyzed is shown. (Scale bars: 50 µm.) (*B*) The plot shows the proportion of total GC PH3 Ser-10$^{+}$ B cells that are localized in the LZ compartment of organized GCs. PH3 Ser-10–positive GC B cells from *A* were counted in LZ and DZ compartments from 104 control (1,039 cells) and 48 CXCL12$^{gagtm}$ GCs (658 cells) and plotted as the percentage of LZ-localized PH3 Ser-10$^{+}$ cells in individual organized GCs. Data pooled from two independent experiments. Red bars show the median; statistical significance was determined by Mann–Whitney test. (*C*) Splenic GC B cells from a pool of three control (*Upper*) and 3 CXCL12$^{gagtm}$ (*Lower*) mice 7 d after SRBC immunization were assessed for PH3 Ser-10, DNA content, CD86 and CXCR4 expression. Data are from one representative experiment out of two. *Upper Left* plots are negative controls with secondary antibody alone.

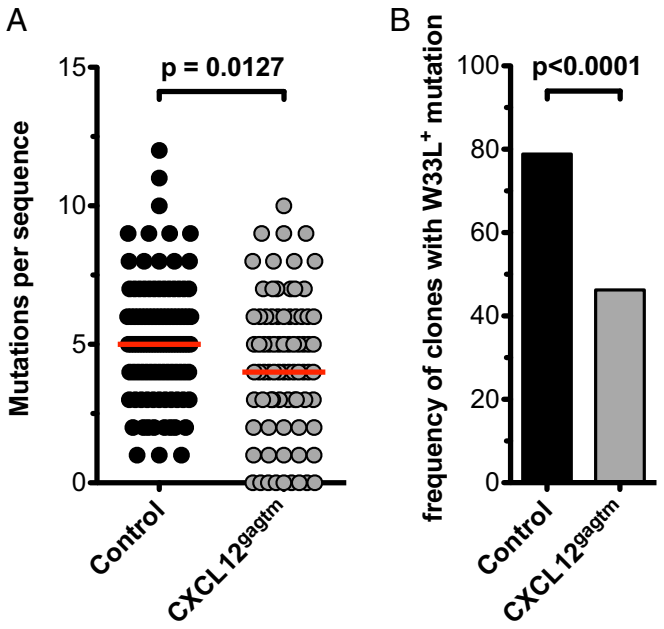


**Fig. 4.** Somatic hypermutation in GC B cells. (*A*) $V_H$186.2 gene mutations in $\lambda1^+$ IgG1$^+$ GC B cells from control and CXCL12$^{gagtm}$ mice on day 13 after immunization with $NP_{35}$-CGG. Data are grouped from two independent experiments, each including three control and three CXCL12$^{gagtm}$ mice. Results are presented as number of mutations per sequence. A total of 104 control and 80 CXCL12$^{gagtm}$ sequences were analyzed. Red bars indicate the median. Statistical significance determined by Mann–Whitney test. (*B*) Frequency of clones with the W33L substitution in the $V_H$186.2 gene from *A*. Statistical significance determined by Fisher's exact test.

To examine the DZ or LZ phenotype of the PH3$^+$ cells, we assessed the expression levels of CD86 and CXCR4 and DNA content by flow cytometry (Fig. 3*C*). DNA content measurement revealed that, among cells in G1 phase, the frequencies of LZ (33.0%) and DZ (46.6%) B cells were comparable with the frequencies observed in the total GC gate (30.3% LZ, 54.5% DZ) (Fig. 1*A*). Consistent with previous findings (19), cells in the G2/M phase of cell cycle constituted ∼8% of total GC B cells and were strongly enriched in cells displaying DZ phenotype in both control (73.2%) and mutant (65.8%) mice (Fig. 3*C*). This enrichment was even more marked among PH3 Ser-10$^+$ cells and constituted 77.5% and 75.7% for control and CXCL12$^{gagtm}$ mice, respectively. The degree of enrichment for DZ cells among PH3 Ser-10$^+$ GC B cells is likely to be even higher because, since DZ and LZ cells are not totally separated by CXCR4/CD86 staining, some DZ cells may fall in the LZ gate when this gate is defined on total GC cells. Similar results were obtained with an antibody specific for phosphorylated H3 at position Ser-28 (Fig. S4). We further analyzed the relationship between B-cell position and cell-cycle status by pulse labeling the dividing cells with 5-bromo-2′-deoxyuridine (BrdU), followed by flow cytometry and histological analysis. Five hours after BrdU injection, positive GC B cells locate to the DZ (26). We therefore examined the phenotype and localization of BrdU-labeled GC B cells 5 h after a single BrdU pulse. This analysis revealed that BrdU$^+$ cells constituted ∼35% of total GC B cells and were strongly enriched in cells with a DZ phenotype, both in control and mutant mice (Fig. S5). Histological analysis of GCs revealed that, in control mice, BrdU$^+$ cells were found mainly in the DZ compartment, as described (26), whereas, in mutant mice, a fraction of BrdU-labeled cells were found in the LZ (Fig. S5*B*). Thus, in CXCL12$^{gagtm}$ mice, some cells with a DZ phenotype, which include a fraction of PH3$^+$ cells in mitosis and a fraction of BrdU$^+$ cells, are mislocalized to the LZ.

**Somatic Hypermutation and Affinity Maturation.** To determine whether lack of CXCL12 immobilization affects somatic mutation in GC B cells, we isolated $\lambda1^+$ IgG1$^+$ GC B cells from control and CXCL12$^{gagtm}$ mice on day 13 after immunization with NP-CGG and sequenced a region of 294 bp of the $V_H$186.2 gene encompassing CDR1 and CDR2. NP-CGG elicits a strong humoral immune response dominated by λ1-expressing B cells carrying the heavy-chain gene $V_H$186.2 (27, 28). Furthermore, a mutation in position 33 of the $V_H$186.2 gene, resulting in the W33L amino acid substitution, confers a 10-fold increase in the affinity of the B cell receptor (BCR) for the hapten 4-hydroxy-3-nitrophenyl acetyl (NP) (29). Sequencing analysis of the $V_H$186.2 gene in GC B cells revealed that the overall number of mutations per sequence was lower in CXCL12$^{gagtm}$ than in control GC B cells. The median number of mutations in control sequences was five, but only four in sequences from mutant mice, with nine sequences from the CXCL12$^{gagtm}$ GC showing no mutations (Fig. 4*A*). Furthermore, the fraction of clones carrying the W33L substitution, which confers high-affinity to NP, was also lower among CXCL12$^{gagtm}$ GC B cells (46.2%) than in control GC B cells (78.8%) (Fig. 4*B*). Overall, these results indicate that disrupted CXCL12 binding to HS affects the selection of high-affinity clones and the accumulation of somatic mutations in GC B cells.

To explore the consequences of the reduced frequency of B cells with the W33L substitution in CXCL12$^{gagtm}$ mice, we studied affinity maturation. We determined the titer and the affinity of serum immunoglobulins after immunization with NP-CGG. As expected, the affinity of NP-specific antibodies was lower in the CXCL12$^{gagtm}$ mice, compared with controls (Fig. 5). Therefore, CXCL12 immobilization on HS is important for selection of high-affinity mutants, and, when the formation of a fixed CXCL12 gradient is prevented, affinity maturation is impaired and the humoral immune response is suboptimal.

## Discussion

Our results reveal the importance of CXCL12 immobilization in the quality of the humoral immune response. During the GC reaction, immobilized CXCL12 forms a fixed gradient with higher concentration of the chemokine in the DZ (11). Opposing gradients of CXCL12 and CXCL13 allow B cells to migrate between the DZ and the LZ, by alternating expression of CXCR4. B cells selected in the LZ for higher affinity to antigen return to the DZ where they undergo further rounds of proliferation and somatic mutation, before returning to the LZ for additional cycles of selection (19). Disruption of CXCL12 binding to HS prevents the

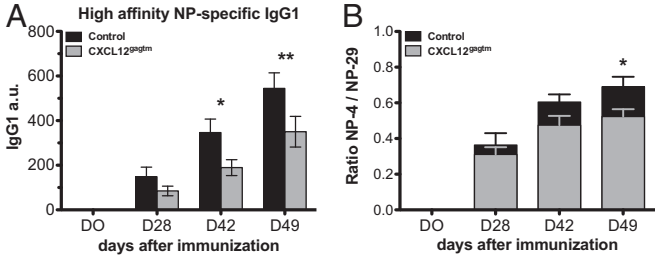


**Fig. 5.** Impaired affinity maturation in CXC12$^{gagtm}$ mice. (*A*) ELISA for high-affinity $NP_4$-specific IgG1 in serum from control and CXC12$^{gagtm}$ mice at the indicated time points after immunization with $NP_{35}$-CGG. (*B*) Ratio of $NP_4$- and $NP_{29}$-specific IgG1 titers. Data are from one representative experiment out of two and are presented as mean ± SEM from four control and five CXC12$^{gagtm}$ mice per time point. *$P < 0.05$; **$P < 0.01$ as determined by the two-way ANOVA test.

establishment of the fixed gradient needed to direct cells selected in the LZ back to the DZ, thus impairing the mechanism of step-wise selection for cells carrying increasing affinity to antigen. As we show in this work, disrupted binding of CXCL12 to HS affects neither the magnitude nor kinetics of the GC reaction, nor the frequency of centroblasts in the GC. Our observations are consistent with reports where GC reaction was studied in CXCR4-deficient mice (11, 25) and suggest that the magnitude of the GC responses may depend on factors other than immobilized CXCL12.

Despite of the comparable magnitude and kinetics of the GC reaction, the structural organization of the splenic GC was significantly affected in mutant animals. The majority of GCs from CXC12$^{gagtm}$ mice showed disrupted organization with no evidence of LZ/DZ polarity. This observation cannot be explained by sectioning artifacts because, although some organized GCs could be sectioned entirely through the FDC-rich area such that they would appear as the disorganized GCs, the overall frequency of such occurrences is expected to be similar in control and mutant mice. Although, in control mice, we observed ∼24% of disorganized GCs, a fraction comparable with the previous large-scale confocal imaging studies in immunized mice (30), a significantly higher proportion of disorganized GCs were observed in the spleens of CXC12$^{gagtm}$ mice. The structure of these disorganized GCs resembled that observed in CXCR4 deficiency (11, 25), suggesting that B-cell responsiveness to immobilized, but not free, CXCL12 contributes to efficient organization of GCs.

It has been suggested that centroblasts residing in the DZ are larger than the LZ centrocytes (21). Although this morphological difference between the two types of the cells was recently questioned (19), our study clearly confirmed significant size differences of GC B cells in the different compartments of control mice. We also show that, in contrast to normal mice, the surface areas of LZ and DZ B cells in CXC12$^{gagtm}$ mice were comparable because of the increased size of B cells in the LZ, suggesting that the localization of larger centroblasts could be defective due to the disrupted binding of CXCL12 to HS. Indeed, analysis of the localization of mitotic cells in mutant mice revealed that they were equally distributed between the LZ and DZ compartments in splenic GCs. Although we also observed mitotic cells in the LZ of control GCs, their numbers were significantly lower (∼30% of all mitotic GC B cells in control compared with 62% in mutant GCs). Therefore, our studies provide quantitative measure and confirm previous observations (25) that some GC B cells undergo mitosis in the LZ, but at a significantly reduced frequency compared with DZ. They also show that disrupted CXCL12 binding to HS prevents efficient trafficking of B cells between the two compartments because the mislocalized cells maintain their morphological (cell size), phenotypic (CD86$^{low}$, CXCR4$^{high}$), and mitotic status. Our findings are compatible with the observation that the DZ and LZ programs are cell-intrinsic and position-independent (25).

The fine-tuned migration of B cells between GC compartments seems to play a general role in the proper accumulation of somatic mutations and affinity maturation. Indeed, the analysis of somatic hypermutation in control and mutant mice revealed that the median number of mutations, the overall mutation frequency, and the number of mutations per sequence in GC B cells are significantly smaller in mutant mice. Furthermore, clones carrying the W33L substitution, characteristic of high-affinity anti-NP antibodies, were also significantly less represented among CXCL12$^{gagtm}$ GC B cells. Consequently, the reduced frequency of high-affinity B cells was reflected in impaired affinity maturation in the CXCL12$^{gagtm}$ mice. We propose that, in CXCL12$^{gagtm}$ mice, when LZ B cells up-regulate CXCR4, they are no longer able to efficiently return to the DZ to introduce more mutations in their Ig genes. Thus, when CXCL12 is not immobilized, B cells with higher affinity antibodies are no longer favored for further rounds of proliferation. Taken together, our results show that effective affinity maturation and optimal humoral immune responses require GC B-cell responsiveness to immobilized, but not free, CXCL12.

## Materials and Methods

**Mice and Immunizations.** CXCL12$^{gagtm}$ mice (8) and littermate controls (all backcrossed to C57BL/6 mice for at least seven generations) 8 to 12 wk old were bred at the Institut Pasteur. Mice were immunized i.p. with 300 μL of SRBC in alsever solution (Eurobio), or $NP_{35}$-GCC (100 μg per mouse; Biosearch Technologies) mixed with 50% (vol/vol) alum (Thermo Scientific). All animal procedures were approved by the Pasteur Institute Safety Committee and conducted according to French and European Community institutional guidelines.

**GC Analysis.** GC were analyzed by flow cytometry after staining splenocytes with antibodies to CD19, IgD, CD38, CD95, CD86, and CXCR4. Immunohistology was performed on 150-μm-thick spleen sections obtained using a vibration-blade microtome. Immunofluorescence images were acquired on a spinning-disk microscope and processed using ICY software (20, 31).

**Antibodies.** All antibodies used in this work are listed in Table S1.

**Sequence Analysis.** The $V_H$186.2 gene was sequenced from the DNA of sorted splenic CD19$^+$ IgD$^-$ CD95$^+$ CD38$^-$ IgG1$^+$ λ1$^+$ cells on day 13 after $NP_{35}$-CGG immunization. PCR products were gel-purified, cloned, and sequenced. The $V_H$186.2 gene was identified by BLAST using the intron sequence upstream of the VH gene and confirmed by BLAST of the VH exon sequence to the mouse genome database and the ImMunoGeneTics (IMGT) database (mouse IMGT/V-QUEST; the alignment tool can be found at www.imgt.org/IMGT_vquest/vquest?livret=0&Option=mouseIg).

**Affinity Maturation and Serum Antibody Analysis.** Serum from $NP_{35}$-CGG–immunized mice was collected at several time points after immunization, and both high-affinity (anti-$NP_4$) and low-affinity (anti-$NP_{29}$) IgG1 antibody titers were determined by ELISA using standard procedures. The plates were standardized using pooled sera from hyperimmunized C57BL/6 mice.

Additional information can be found in *SI Materials and Methods*.

**ACKNOWLEDGMENTS.** We thank A. Cumano for critical reading of the manuscript, advice, and helpful discussions; H. Mouquet for critical reading of the manuscript; G. Millot and V. Rouilly for advice on the statistical analysis; L. Fiette, P. Flamant, and P. Ave for advice and help on histological preparations; the staff of the animal facility of the Pasteur Institute for mouse care; and the Imagopole platform for advice and access to microscopes. This work was supported by the Pasteur Institute, INSERM, and the Agence Nationale de Recherche (Grant "ChemImmun").

1. Cyster JG (1999) Chemokines and cell migration in secondary lymphoid organs. *Science* 286(5447):2098–2102.
2. Campbell JJ, et al. (1998) Chemokines and the arrest of lymphocytes rolling under flow conditions. *Science* 279(5349):381–384.
3. Laguri C, Arenzana-Seisdedos F, Lortat-Jacob H (2008) Relationships between glycosaminoglycan and receptor binding sites in chemokines-the CXCL12 example. *Carbohydr Res* 343(12):2018–2023.
4. Schumann K, et al. (2010) Immobilized chemokine fields and soluble chemokine gradients cooperatively shape migration patterns of dendritic cells. *Immunity* 32(5):703–713.
5. Laguri C, et al. (2007) The novel CXCL12gamma isoform encodes an unstructured cationic domain which regulates bioactivity and interaction with both glycosaminoglycans and CXCR4. *PLoS One* 2(10):e1110.
6. Rueda P, et al. (2008) The CXCL12gamma chemokine displays unprecedented structural and functional properties that make it a paradigm of chemoattractant proteins. *PLoS One* 3(7):e2543.
7. O'Boyle G, Mellor P, Kirby JA, Ali S (2009) Anti-inflammatory therapy by intravenous delivery of non-heparan sulfate-binding CXCL12. *FASEB J* 23(11):3906–3916.
8. Rueda P, et al. (2012) Homeostatic and tissue reparation defaults in mice carrying selective genetic invalidation of CXCL12/proteoglycan interactions. *Circulation* 126(15):1882–1895.
9. Ma Q, et al. (1998) Impaired B-lymphopoiesis, myelopoiesis, and derailed cerebellar neuron migration in CXCR4- and SDF-1-deficient mice. *Proc Natl Acad Sci USA* 95(16):9448–9453.
10. Nagasawa T, et al. (1996) Defects of B-cell lymphopoiesis and bone-marrow myelopoiesis in mice lacking the CXC chemokine PBSF/SDF-1. *Nature* 382(6592):635–638.

11. Allen CD, et al. (2004) Germinal center dark and light zone organization is mediated by CXCR4 and CXCR5. *Nat Immunol* 5(9):943–952.
12. Cyster JG (2003) Homing of antibody secreting cells. *Immunol Rev* 194:48–60.
13. Hargreaves DC, et al. (2001) A coordinated change in chemokine responsiveness guides plasma cell movements. *J Exp Med* 194(1):45–56.
14. Shlomchik MJ, Weisel F (2012) Germinal center selection and the development of memory B and plasma cells. *Immunol Rev* 247(1):52–63.
15. Pereira JP, Kelly LM, Cyster JG (2010) Finding the right niche: B-cell migration in the early phases of T-dependent antibody responses. *Int Immunol* 22(6):413–419.
16. Crouch EE, et al. (2007) Regulation of AID expression in the immune response. *J Exp Med* 204(5):1145–1156.
17. Storck S, Aoufouchi S, Weill JC, Reynaud CA (2011) AID and partners: For better and (not) for worse. *Curr Opin Immunol* 23(3):337–344.
18. Calado DP, et al. (2012) The cell-cycle regulator c-Myc is essential for the formation and maintenance of germinal centers. *Nat Immunol* 13(11):1092–1100.
19. Victora GD, et al. (2010) Germinal center dynamics revealed by multiphoton microscopy with a photoactivatable fluorescent reporter. *Cell* 143(4):592–605.
20. de Chaumont F, et al. (2012) Icy: An open bioimage informatics platform for extended reproducible research. *Nat Methods* 9(7):690–696.
21. MacLennan IC (1994) Germinal centers. *Annu Rev Immunol* 12:117–139.
22. Nieuwenhuis P, Opstelten D (1984) Functional anatomy of germinal centers. *Am J Anat* 170(3):421–435.
23. Goto H, et al. (1999) Identification of a novel phosphorylation site on histone H3 coupled with mitotic chromosome condensation. *J Biol Chem* 274(36):25543–25549.
24. Prigent C, Dimitrov S (2003) Phosphorylation of serine 10 in histone H3, what for? *J Cell Sci* 116(Pt 18):3677–3685.
25. Bannard O, et al. (2013) Germinal center centroblasts transition to a centrocyte phenotype according to a timed program and depend on the dark zone for effective selection. *Immunity* 39(5):912–924.
26. Allen CDC, Okada T, Tang HL, Cyster JG (2007) Imaging of germinal center selection events during affinity maturation. *Science* 315(5811):528–531.
27. Cumano A, Rajewsky K (1985) Structure of primary anti-(4-hydroxy-3-nitrophenyl) acetyl (NP) antibodies in normal and idiotypically suppressed C57BL/6 mice. *Eur J Immunol* 15(5):512–520.
28. Cumano A, Rajewsky K (1986) Clonal recruitment and somatic mutation in the generation of immunological memory to the hapten NP. *EMBO J* 5(10):2459–2468.
29. Allen D, Simon T, Sablitzky F, Rajewsky K, Cumano A (1988) Antibody engineering for the analysis of affinity maturation of an anti-hapten response. *EMBO J* 7(7):1995–2001.
30. Wittenbrink N, Klein A, Weiser AA, Schuchhardt J, Or-Guil M (2011) Is there a typical germinal center? A large-scale immunohistological study on the cellular composition of germinal centers during the hapten-carrier-driven primary immune response in mice. *J Immunol* 187(12):6185–6196.
31. Dufour A, Meas-Yedid V, Grassart A, Olivo-Marin J-C (2008) Automated quantification of cell endocytosis using active contours and wavelets. *Proceedings of the Nineteenth International Conference on Pattern Recognition* (IEEE, New York), pp 1–4.